Available online at www.sciencedirect.com
SCIENCE DIRECT
Forest Ecology and Management 225 (2006) 378–390
Forest Ecology and Management
www.elsevier.com/locate/foreco

Modeling forest stand structure attributes using Landsat ETM+ data: Application to mapping of aboveground biomass and stand volume

R.J. Hall [a,*], R.S. Skakun [a], E.J. Arsenault [a], B.S. Case [b]

[a] *Natural Resources Canada, Canadian Forest Service, Northern Forestry Centre, Edmonton, Alta., Canada T6H 3S5*
[b] *Environment, Society, and Design Division, Lincoln University, P.O. Box 84, Canterbury, New Zealand*

Received 8 March 2005; received in revised form 5 January 2006; accepted 9 January 2006

Abstract

Maps of aboveground biomass (AGB) and stand volume are of interest to determine their magnitude and spatial distribution over forested areas, and required for input to forecasting carbon budgets and ecosystem productivity. Deriving estimates of AGB and volume requires information about species composition and forest stand structure. This paper introduces a method called BioSTRUCT (*Bio*mass estimation from stand *STRUCT*ure), which is based on georeferenced field plots to generate empirical relationships between continuous estimates of forest structure attributes and remote sensing image data represented as spectral response variables. In this study, height and crown closure attributes were modeled from Landsat ETM+ image and field plot data. These modeled attributes were then used as inputs to stand-level models of AGB and volume. The image height model had an adjusted R^2 of 0.65 from ETM+ bands 3, 4, and 5. Likewise, the crown closure model had an adjusted R^2 of 0.57 using ETM+ bands 3, 4, and 7. Average AGB estimates were within 4 tonnes/ha and stand volume was within 4 m^3/ha of field plot values, statistically similar to a validation sample data set for both AGB ($p = 0.61$) and stand volume ($p = 0.65$), and within the range of previous published studies. Field plot distribution, error propagation, and extending models over multiple images were identified as factors requiring further investigation in order to apply BioSTRUCT over larger geographic areas.

Keywords: Forest biomass; Stand volume; Landsat; Stand structure; Carbon; Forest inventory; BioSTRUCT

1. Introduction

Information about aboveground biomass (AGB) is necessary for estimating and forecasting ecosystem productivity, carbon budgets, nutrient allocation, and fuel accumulation (Brown et al., 1999; Kurz and Apps, 1999; Price et al., 1999; Zheng et al., 2004). Being able to accurately estimate biomass is therefore important to assess the role of forests in the global carbon (C) cycle, particularly when defining its contribution toward sequestering carbon (Brown, 2002; Parresol, 1999). Biomass is also considered a useful indicator of structural and functional attributes of forest ecosystems across a wide range of environmental conditions (Brown et al., 1999). Toward this end, the general lack of accurate spatial forest biomass data has been considered one of the most persistent uncertainties concerning global C budgets (Harrell et al., 1995).

Notably, inventory data from field plots have been the most practical means for estimating AGB (Brown, 2002), whereby measurements of tree size and stand structure along with statistical models are used in estimation of tree and stand biomass (Parresol, 1999; Fournier et al., 2003; Jenkins et al., 2003). Several studies have applied spatial inventory data comprising forest cover polygons in the production of biomass maps. Bonner (1985) compiled the first national forest biomass inventory in Canada that was updated by Penner et al. (1997). Stand volume was converted to aboveground forest biomass to map its spatial distribution over forests of the eastern United States of America (Brown et al., 1999). More recently, as part of the Earth Observation for Sustainable Development of Forests (EOSD) project (Wood et al., 2002) for forest biomass (Luther et al., 2002), field plot information was used to scale AGB from the tree to the stand level of which a map could then be derived from applying the estimates of stand attributes to spatial inventory data (Fournier et al., 2003). Extending inventory data into maps of forest biomass is challenging and influenced by at least these five factors: (1) ecological differences over large areas, (2) variation in the age of the data (Brown, 2002), (3)

* Corresponding author. Tel.: +1 780 435 7209; fax: +1 780 435 7359.
E-mail address: rhall@nrcan.gc.ca (R.J. Hall).

0378-1127/$ – see front matter.
doi:10.1016/j.foreco.2006.01.014

differences in inventory classification systems across the country (Gillis and Leckie, 1993), (4) geographically scattered biomass source data and equations (Ter-Mikaelian and Korzukhin, 1997), and (5) availability of inventory-based biomass estimates for only managed forest areas. These factors create data gaps and variations in estimates that can compromise inferences regarding measures of achieving forest management or ecosystem sustainability goals.

A logical extension of conventional tree and stand biomass models is to adapt them to use remote sensing as input data. Several studies have mapped AGB in boreal, temperate, and tropical environments using remote sensing data. Relationships have been developed between forest biomass and vegetation indices using Landsat Thematic Mapper (TM) (Sader et al., 1989; Lee and Nakane, 1997; Zheng et al., 2004) and Synthetic Aperature Radar backscatter data (Kasischke et al., 1994; Wang et al., 1994). In India, a forest type crown cover map, was produced from IRS-1A data for biomass mapping (Tiwari, 1994). Relationships between Normalized Difference Vegetation Index values from the Advanced Very High Resolution Radiometer and woody biomass estimates from forest inventories of six countries (Canada, Finland, Norway, Russia, USA, and Sweden) were used to map biomass of boreal and temperate forests in the Northern Hemisphere (Dong et al., 2003). These studies have all mapped AGB, and the use of remote sensing data was reported to varying degrees of success.

Considerable efforts have been directed at using remote sensing to estimate forest stand attributes of cover, age, crown closure, and height (Franklin, 2001). Generating a continuous variable model (CVM) is one approach based on an empirical model for continuous estimation of stand attributes (Cohen et al., 2001). While highly precise estimates of stand attributes would not necessarily be expected from remote sensing data, reported estimates have been within the vicinity of expected values from studies in Finland (Hyyppä et al., 2000), United States (Cohen et al., 2001), and Canada (Hansen et al., 2001; Gerylo et al., 2002). Biomass and stand volume at tree or stand levels are highly correlated (Bonner, 1985; Penner et al., 1997), and assessing the degree to which both can be estimated and mapped are useful to the forestry community. If reasonable estimates of stand attributes were derived from remote sensing, then these estimates could be used as inputs to models that estimate AGB and stand volume.

This paper introduces a method called BioSTRUCT (*Bio*mass from modeling stand *STRUCT*ure) that estimates AGB or stand volume using a two-step process that (a) applies the CVM approach to the remote sensing image to estimate stand attributes, and (b) uses the stand attributes in empirical models to estimate AGB and stand volume. The objectives of this study were to describe BioSTRUCT and to evaluate proposed improvements to the CVM approach by incorporating refinements with regards to image segmentation, pixel sampling and modeling. Addressing these objectives entailed two hypotheses. First, stand structural model predictive performance was hypothesized to be improved from image segmentation compared to sampling all pixels within a more conventional 3×3 pixel image window. Second, the integration of field-based AGB and stand volume models with remote sensing of structure was hypothesized to be more accurate when compared to use of spatial inventory data alone. This study therefore assessed the results from integrating field and remote sensing data and compared them to those generated from the more frequently used approach of inventory data (Fournier et al., 2003).

2. Methods

2.1. Study area

The study area comprises a 2600 km^2 area in west-central Alberta with corners located approximately at 53.35°N, 116.50°W on the northeast, and at 53.00°N, 117.50°W on the southwest, and is situated immediately southeast to the town of Hinton (Fig. 1). Within the study area are four ecoregions: Upper Boreal-Cordilleran (Upper Foothills), Lower Boreal-Cordilleran (Lower Foothills), Subalpine, and Montane, which occupy 68, 21, 10, and 1% of the total area, respectively (Achuff, 1992). The terrain ranges from gently undulating to highly dissected, strongly rolling, and hilly topography. Elevations range from 1070 m above sea level in the east to 1725 m at the extreme west.

The Alberta Vegetation Inventory (AVI) (Alberta Environmental Protection, 1991) for the study area was based on interpretation of 1:15,000 black and white aerial photographs acquired during the 1993 field season with Agfa Aviphot Pan 200 aerial film. Based on the AVI, 78% of the total area was occupied by pure stands of lodgepole pine (*Pinus contorta* Dougl.), white spruce (*Picea glauca* (Moench) Voss) and black spruce (*Populus balsamifera* L.), followed by 11% shrub, 8% trembling aspen (*Populus tremuloides* Michx.) and balsam

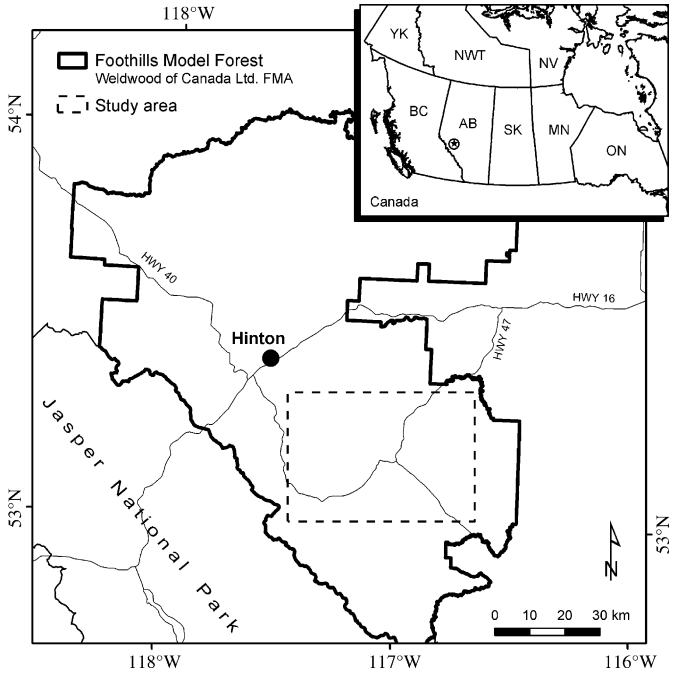

Fig. 1. Map of study area located southeast to the town of Hinton, in west-central Alberta.

poplar (*P. balsamifera* L.), and the remainder consisting of water and other species (e.g., *Larix laricina* (Du Roi) K. Koch) in 1% increments. Due to the obvious dominance of conifer species in the study area, this study focused on method development to estimate AGB and stand volume for the conifer component.

2.2. Field data

The field data for the study was acquired from permanent growth sample (PGS) plots collected from 1990 to 2000. PGS plots were established in clusters of four plots every 3 km to monitor the amount and rate of forest growth and yield (Weldwood of Canada Limited Hinton Division, 1999). Within the cluster, the PGS plots were positioned at 45° and 100 m from the cluster location resulting in a physical spacing of approximately 150 m from centre to centre between each plot. The general size was 0.08 or 0.04 ha, depending on the year of establishment. The PGS plots were then compiled and stratified into coniferous, deciduous, and mixed species groups, using the decision rule that dominant species occupying greater than or equal to 80% of stand composition was considered a pure stand. Based on this decision rule, there were 153 PGS plots in the coniferous species group.

The standard PGS plot data collection protocol for selected trees (a commercial species equal or above 1.3 m height) included: species, percent species composition, stand height (measured to the nearest metre), diameter breast height (dbh, cm), age, and an AVI field call of stand composition. Tree heights were measured to the tallest live portion of the crown using a Vertex or laser height finder. Age measurements were taken by coring selected trees and average stand height was computed by averaging the Lorey heights of trees within a given plot (Philip, 1994). Since continuous crown closure measurements were not collected at the PGS plots, 80 independent field measures of crown closure representing the coniferous species group were also collected in the study region using a protocol similar to Hall et al. (2003).

Plots were stratified into model calibration and validation samples (Fig. 2). A 75% random sample of the data was used for model calibration of height and crown closure, and the remaining 25% of the sample was used for independent validation. From this procedure, a total of 115 height plots and 60 crown closure plots were used for model calibration, with 38 height plots and 20 crown closure plots remaining for independent model validation. Descriptive statistics were calculated for the model calibration and validation data sets and an *F*-test was conducted to determine their statistical similarity. All statistical tests in this study were conducted at the 5% level of significance.

2.3. Estimating biomass and volume from the field data

Generalized, allometric tree biomass equations ($AGBi = aDBH^b$) are often used in biomass studies (Crow and Laidly, 1980; Wang et al., 2002; Jenkins et al., 2003). This model form was used to generate biomass data for a range of 10 species in the boreal forest regions of the Prairie Provinces (Singh, 1982), Northwest Territories (Singh, 1984), and the Yukon Territory (Manning et al., 1984). Tree-level biomass was summed for each tree in the PGS plot and consequently converted to a stand-level total AGB density (tonnes/ha). To relate the AGB computed at each PGS plot to stand attributes, it was modeled as a function of stand height and crown closure derived from the field for the coniferous species (Fig. 2). A model form was selected to generate an approximate linear relationship between AGB (Y) with stand height (X_1) and crown closure (X_2) while accounting for possible problems of error variance heteroscedasticity in the overall regression model $Y^{1/3} = a + b \times \ln X_1 + c \times X_2$. Similarly, provincial taper models were used to estimate total volume of individual trees (Huang, 1994) in each PGS plot that were then summed to obtain a total volume estimate. The total volumes were divided by the plot area and extrapolated to a per hectare basis in order to estimate volume in cubic metres per hectare (m^3/ha). The volume per hectare estimate was then modeled as a function of stand height and crown closure using the same model form as for AGB. Overall, the AGB and stand volume models were generated from 115 PGS plot samples and then assessed by their adjusted R^2 and root mean square error (RMSE) values. The predictive performance of these model functions was also tested through comparison of plot sample and model predicted values from the 38 validation samples in a *T*-test.

2.4. Landsat ETM+ data

Landsat ETM+ satellite data (WRS-2: Path 45 and Row 23) was acquired for August 23, 2002, orthorectified and georeferenced to a UTM Zone 11 projection based on the NAD83 datum. A Top-of-Atmosphere Reflectance (TOAR) correction procedure, based upon Markham and Barker (1986) was then applied to all Landsat ETM+ bands except the thermal (Peddle et al., 2003). The TOAR procedure corrects for variations in solar illumination and assumes a uniform atmosphere within the image. The image was transformed from raw digital numbers to TOAR reflectance values using image calibration values, radiometric ancillary information, solar zenith angle, and Earth–Sun distance measurements.[1] A dark-object subtraction procedure was also applied to reduce path radiance effects in the visible bands (Teillet and Fedosejevs, 1995).

2.5. Landsat ETM+ band selection for modeling stand structure

A field plot located within a stand was nominally the size of 1/2 to 1 image pixel. For the model calibration sample, the pixel values within the 3 × 3 pixel window surrounding the centre pixel of the field plot were averaged for each Landsat ETM+ band. Averaging spectral values within a window surrounding the

[1] Landry, R., December 2004. Personal communications. Canada Centre for Remote Sensing.

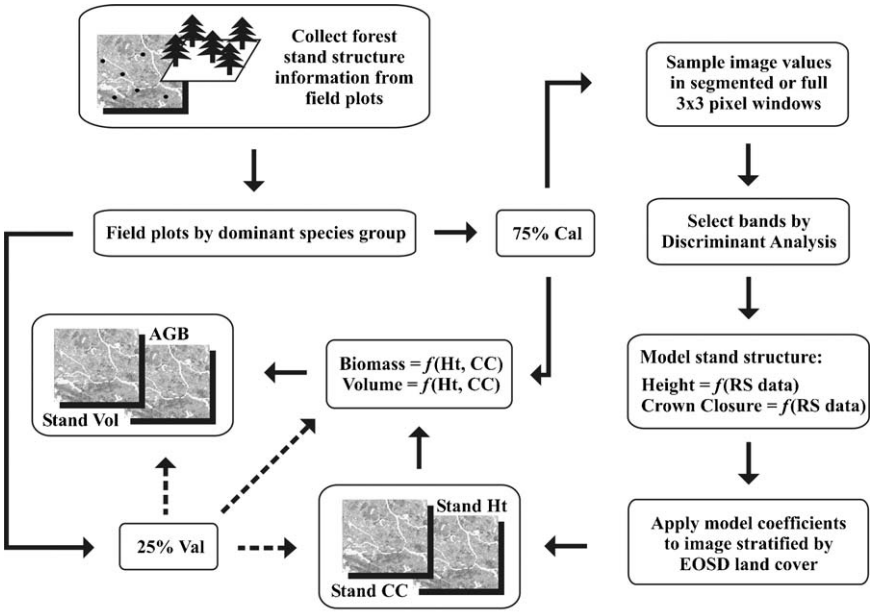

Fig. 2. Flow chart of methods for BioSTRUCT.

centre of the plot is thought to reduce sampling error in the case of spatial mis-registration of the image. This approach, however, may return false results due to the influence of edge effects from cutblocks, roads or spectrally different cover types. An image segmentation procedure was introduced to remove pixels attributable to these features. In this procedure, the average heterogeneity of the image was reduced by segmenting features based upon similarities in shape, colour and size. For this study, the segmentation parameter settings from eCognition v3.0 (Definiens Imaging, 2002) were scale (10), colour (0.6), shape (0.4), smoothness (0.5), and compactness (0.5). The image segments containing field plots were then intersected with the 3×3 pixel windows resulting in a mask of homogeneous pixel values for each plot (Fig. 3). The mean pixel value for each image band was then computed from these homogeneous pixels.

Pearson's product moment correlation coefficients (R) were calculated between field-based stand height and crown closure and the mean Landsat ETM+ band and Tassel Cap (Huang et al., 2002) brightness, greenness, and wetness values for the full 3×3 window and the intersected window. Inferences were made about which Landsat ETM+ or Tassel Cap transformed image bands were most correlated to stand height and crown closure, and whether image segmentation made any difference to the magnitude of these coefficients.

Discriminant function analysis, a procedure often used in image feature selection (Landgrebe, 2000), was used to select the Landsat ETM+ bands to model stand height and crown closure. Using a forward stepwise method, the Landsat ETM+ bands that contributed most to height or crown closure discrimination was added until its statistical significance was lower than a user-defined *F-to-remove* value (*F-to-remove* = 3.0). These image bands were subsequently used in the modeling and mapping of stand structure.

2.6. Mapping stand structure from remote sensing

Stand height and crown closure as a function of Landsat ETM+ spectral response was modeled using multivariate regression. Non-linear regression models were generated for stand height and crown closure using the calibration sample data and associated mean Landsat ETM+ band values (Oakdale Engineering, 2002). The results of the Landsat ETM+ band selection from the discriminant analysis were used as the independent variables in the modeling exercise. The models producing the highest adjusted R^2 and lowest root mean square error for stand height and crown closure was determined as the best function to model stand structure.

The model form and regression coefficients for stand height and crown closure were then applied to the Landsat ETM+ image (Fig. 2). Coniferous land cover generated as part of the Earth Observation for Sustainable Development of Forests Project (Wulder et al., 2003) was used as a mask so that only pixels representative of coniferous forest would be modeled. The independent sample of validation plots was used to assess the predictive performance of these models.

2.7. Estimation and mapping of biomass and volume

To estimate and map AGB and total volume from the Landsat ETM+ image, the image estimates of stand height and crown closure were used as inputs to the models which estimate volume and biomass (Fig. 2). The validation sample plots were then used to evaluate AGB and total volume from the Landsat ETM+ image estimates of stand height and crown closure. These results were compared with AGB and total volume generated from the AVI inventory data. As a basis for

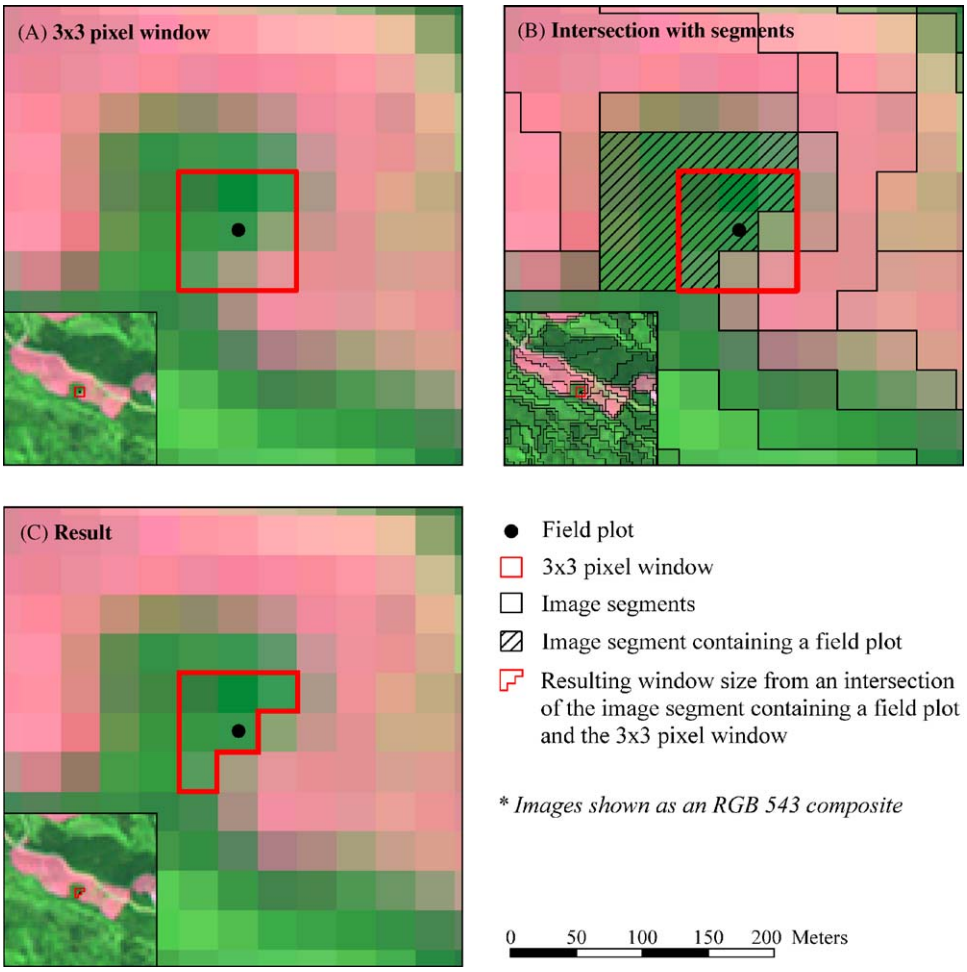

Fig. 3. An illustrative example of the image segmentation procedure for a field plot located near the edge of a cutblock. (A) The objective is to remove the spectrally uncharacteristic pixels (i.e. pink pixels) from the 3 × 3 pixel window surrounding the field plot. (B) Initially, the image is segmented into spectrally homogenous polygon segments, followed by an intersection of the image segment containing the field plot with the 3 × 3 pixel window. (C) The result is a redefined window size that captures the image pixels most representative of the field plot.

comparison, direct estimation models for AGB and volume as a function of Landsat ETM+ bands were compared to models generated from BioSTRUCT. Direct estimation is when the variables of interest, AGB, and volume, are estimated directly from an empirical or statistical model using the Landsat ETM+ bands as predictor variables. Making this comparison demonstrated if advantages occurred from the methods that comprised BioSTRUCT.

3. Results

3.1. Distribution of conifer height, crown closure, biomass, and volume

Conifer stand height and crown closure ranged from 6 to 25 m and 15 to 85%, respectively, which represented a full range of stand structures that occurred in the study area (Table 1). While

Table 1
Descriptive statistics of the model and validation samples for height, crown closure, biomass, and volume estimates

	Height (m)		Crown closure (%)		Biomass (tonnes/ha)		Volume (m^3/ha)	
	Model	Validation	Model	Validation	Model	Validation	Model	Validation
N	115	38	60	20	115	38	115	38
Mean	12.8	14.4	44	42	114.3	114.4	188.5	194.1
S.D.	4.7	5.4	18	19	62.1	60.2	138.5	141.1
Range	19	16	88	79	269	256	625	610
Minimum	6	8	5	4	5	28	7	30
Maximum	25	24	93	83	274	284	632	640

most stands ranged from 8 to 10 m in height and from 30 to 60% in crown closure (Fig. 4a and b), values varied by species. Average stand heights were 12.9 m (standard deviation (S) = 4.8 m) for lodgepole pine, 16.1 m (S = 5.2 m) for white spruce, and 11.2 m (S = 3.5 m) for black spruce. Average crown closure was highest for lodgepole pine (44%, S = 18%), and white spruce (46%, S = 22%), and lowest or most open for black spruce (25%, S = 18%). Given the nominal age of these stands (lodgepole pine, 68 years; white spruce, 108 years; black spruce, 115 years), these values were typical of boreal conifer stands within the Foothills region.[2] The model fitting and validation samples were statistically similar for stand height ($p = 0.324$) and crown closure ($p = 0.853$) suggesting that the validation data sample would be a reasonable sample data set from which to assess model performance.

3.2. AGB and stand volume models

Using the model fitting data set, the following models were derived to estimate AGB and stand volume using stand height and the mid-point of the crown closure from the PGS plot:

$$\mathrm{AGB}^{1/3} = -0.677 + 1.874 \times \ln(\text{height}) + 0.014(\text{crown closure}) \quad (1)$$

$$\mathrm{Volume}^{1/3} = -3.252 + 3.089 \times \ln(\text{height}) + 0.02(\text{crown closure}) \quad (2)$$

The model for AGB resulted in an adjusted $R^2 = 0.70$ with a RMSE = 33.7 tonnes/ha. The model for volume resulted in an adjusted $R^2 = 0.71$ with a RMSE = 74.7 m^3/ha. These models compared favourably to direct estimation models of AGB (adjusted $R^2 = 0.40$; RMSE = 52.7 tonnes/ha) and volume (adjusted $R^2 = 0.30$; RMSE = 110.8 m^3/ha) as a function of Landsat ETM+ bands. These model results also compared favourably to studies that reported larger RMSE values for biomass in Sweden (61.4 tonnes/ha) (Fazakas et al., 1999), Northern Wisconsin (54 tonnes/ha) (Zheng et al., 2004) and Newfoundland (63.6 tonnes/ha) (Luther et al., in press). Similarly, volume values compared favourably to RMSE values reported by Trotter et al. (1997) (>100 m^3/ha) and Fazakas et al. (1999) (121.2 m^3/ha). There was a broad range in AGB and total stand volume values where the conifer stands ranged from 5 to 284 tonnes/ha and 7 to 640 m^3/ha, respectively (Table 1). Based on the field validation sample, the average difference in the model predicted values for AGB and volume was −0.40 tonnes/ha (S = 1.95) and −0.92 m^3/ha (S = 4.40), respectively. These AGB bias results were less than half the size of values reported by Fazakas et al. (1999) (0.9 tonnes/ha) and Tomppo et al. (2002) (1.2 tonnes/ha). Similarly, volume bias results were smaller than those reported by Fazakas et al. (1999) (−1.9 m^3/ha) and Tomppo et al. (2002) (−3.0 m^3/ha). There were no statistical differences in the prediction of AGB ($p = 0.221$) and volume ($p = 0.205$) when compared to the validation sample, and they were much smaller than those computed from direct estimation models where the average difference for AGB and volume was 20.7 tonnes/ha (S = 82.0) and 42.3 m^3/ha (S = 151.3), respectively. The estimation of AGB and volume through stand structure were therefore more favourable than those derived from direct estimation.

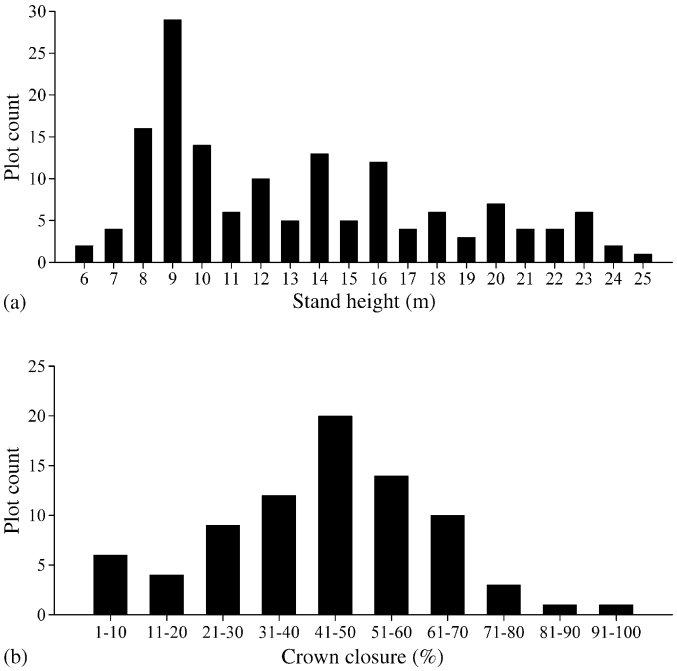

Fig. 4. Distribution of stand structure in the study area depicted by (a) stand height histogram for field plots sampled from 1990 to 2000 (n = 153) and (b) crown closure histogram for field plots sampled in 2002 and 2003 (n = 80).

3.3. Relationships between stand variables and Landsat ETM+ bands

Increases in stand height and crown closure estimates were negatively correlated with ETM+ spectral response for the full 3 × 3 window (Table 2). Consistent with previously reported studies (Gerylo et al., 2002), correlation coefficients for stand height were highest with Landsat ETM+ bands 4 (near-infrared) and 5 (mid-infrared) with R-values of −0.60 ($p = 0.004$) and −0.63 ($p = 0.002$), respectively. Trends for crown closure were similar with the highest correlations from Landsat ETM+ bands 4 and 5, with R-values ranging from −0.58 ($p = 0.005$) to −0.55 ($p = 0.024$), respectively. Correlation coefficients generated from Landsat ETM+ image bands were higher than those generated from Tassel Cap brightness, greenness, and wetness (Table 2).

Segmentation within the 3 × 3 window resulted in consistently higher correlation coefficients than from sampling the full 3 × 3 window (Table 2). Landsat ETM+ bands 4 and 5 resulted in the highest correlations for stand height (R-values of −0.68 ($p = <0.001$) and −0.73 ($p = <0.001$), respectively) and crown closure (R-values of −0.65 ($p = 0.001$) and −0.59

[2] Huang, S., December 2004. Personal communications. Alberta Sustainable Resource Development.

Table 2
Correlation coefficients between height and crown closure plot estimates and image spectral response

	Height				Crown closure			
	3 × 3 window		Segmented window		3 × 3 window		Segmented window	
	R	*p*-Value	*R*	*p*-Value	*R*	*p*-Value	*R*	*p*-Value
ETM+ 1	−0.16	0.393	−0.14	0.411	−0.19	0.326	−0.21	0.185
ETM+ 2	−0.33	0.102	−0.34	0.097	−0.25	0.210	−0.32	0.089
ETM+ 3	−0.54	0.016*	−0.59	0.003*	−0.48	0.039*	−0.50	0.026*
ETM+ 4	−0.60	0.004*	−0.68	<0.001*	−0.58	0.005*	−0.65	0.001*
ETM+ 5	−0.63	0.002*	−0.73	<0.001*	−0.55	0.024*	−0.59	0.002*
ETM+ 7	−0.45	0.028*	−0.45	0.026*	−0.49	0.042*	−0.52	0.020*
Brightness	−0.52	0.013*	−0.58	0.005*	−0.28	0.190	−0.32	0.090
Greenness	−0.53	0.013*	−0.60	<0.001*	−0.09	0.492	−0.16	0.374
Wetness	0.45	0.027*	0.54	0.011*	0.40	0.030*	0.47	0.041*

* Statistically significant at $p = 0.05$.

Table 3
Multivariate regression results for estimating height and crown closure from image spectral response

	Regression parameters ($Y = \exp(B_0 + B_1X_1 + \cdots B_nX_n)$)				Adjusted R^2	RMSE
	B_0	B_1X_1	B_2X_2	B_3X_3		
Ht (m)	4.13	−0.039 (ETM+ 3)	−0.011 (ETM+ 4)	−0.026 (ETM+ 5)	0.65	2.8
CC (%)	5.22	−0.017 (ETM+ 3)	−0.007 (ETM+ 4)	−0.079 (ETM+ 7)	0.57	12.0

All regressions significant at $p = 0.05$.

($p = 0.002$), respectively). The negative correlations for both height and crown closure were consistent with previous reports that suggest as trees age and grow in height, the amount of shadow effects, and leaf area that cover the brighter understory increases, resulting in reduction to overall spectral response (Gemmell, 1995; Franklin et al., 2002). Segmentation resulted in a subset of image pixels that better represented land cover features that were related to the field sample compared to selection from the full 3 × 3 window.

Factors relating to the physical structure of the forest canopy such as height, basal area and biomass are considered best predicted using a combination of visible and middle-infrared Thematic Mapper bands (Jakubauskas and Price, 1997). Given the variable relationships between the Landsat ETM+ image bands and stand height and crown closure, an obvious question was which would be most useful as model predictors of these stand attributes? Based on a forward stepwise discriminant analysis, Landsat ETM+ bands 3, 4, and 5 were selected for stand height and Landsat ETM+ bands 3, 4, and 7 for crown closure. The standardized discriminant function coefficients provided an indicator of the relative importance of the independent variables in predicting the dependent. In the discriminant analysis output for stand height, the standardized discriminant function coefficient values were 0.69 (Landsat ETM+ band 5), 0.61 (Landsat ETM+ band 4), and 0.33 (Landsat ETM+ band 3). For crown closure, the standardized discriminant function coefficient values were 0.97 (Landsat ETM+ band 4), 0.31 (Landsat ETM+ band 3), and 0.25 (Landsat ETM+ 7). Landsat ETM+ band 4 was considered a strong predictor of both stand height and crown closure, similar to other studies reported for modeling stand attributes (Gerylo et al., 2002).

The multivariate exponential regression function resulted in the best model performance for predicting height and crown closure. Using Landsat ETM+ bands 3, 4, and 5 as predictor variables of stand height, the adjusted R^2 was 0.65 with a RMSE of 2.8 m (Table 3). For the exponential model of crown closure using Landsat ETM+ bands 3, 4, and 7, the adjusted R^2 was 0.57 with a RMSE of 12.0%. The models presented in Table 3 were used to generate a height and crown closure image output (Fig. 5). The cutblocks and regenerating stands were easily identified by the darker blue tones, which represented the shorter tree heights and open canopies. The image maps depict the coniferous stands as ranging mostly from 12 to 18 m stand heights with partially closed canopies, which corresponded with stand structure described by the field data (Fig. 4a and b).

Based on the validation sample, the average difference in Landsat ETM+ estimated stand height from the segmented 3 × 3 window was lower, less variable, and not statistically different from field values ($\bar{X} = -0.29$ m, $S = 5.46$ m, $p = 0.746$) compared to stand height estimated from the full 3 × 3 image window ($\bar{X} = -2.74$ m, $S = 8.30$ m, $p = 0.049$). The crown closure estimates from either the segmented or full 3 × 3 window were not statistically different than field values ($p = 0.136$ and 0.121, respectively). The average difference in Landsat ETM+ estimated crown closure was lower, and less variable, however, from the model based on the segmented 3 × 3 window ($\bar{X} = -4.7\%$, $S = 13.5\%$) compared to the full 3 × 3 window ($\bar{X} = -7.7\%$, $S = 21.2\%$).

Stand height and crown closure were best estimated for stands 10–20 m in height that ranged from 31 to 50% crown closure (Fig. 6a and b). These same attributes were overestimated at the low end for stand height less than 10 m and 31% crown closure,

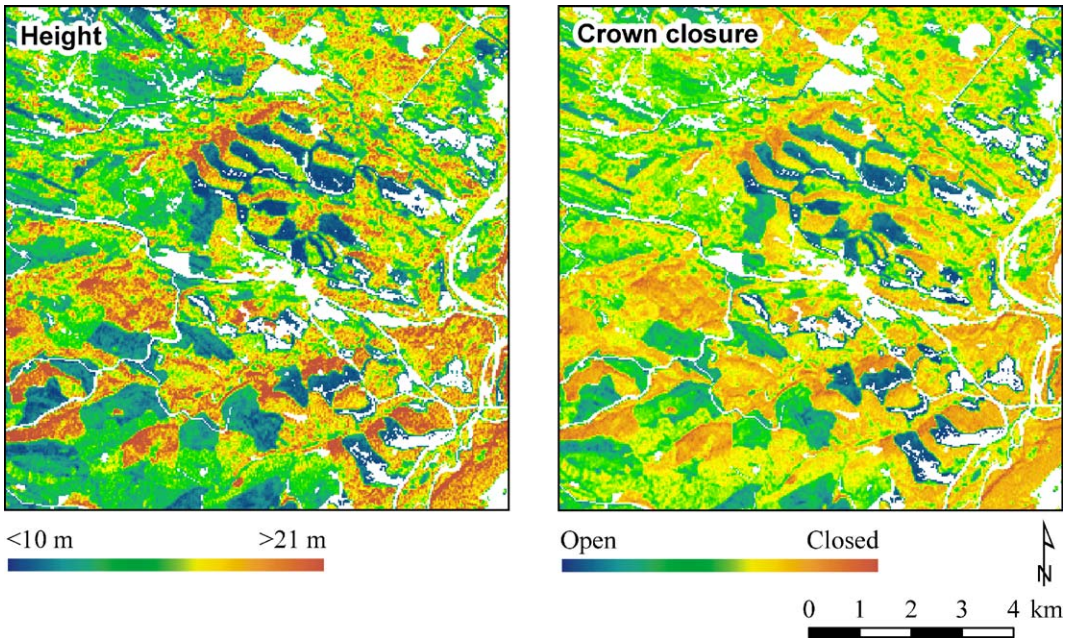

Fig. 5. Modeled height and crown closure estimates for a subset region of the study area. Cutblocks and regenerating stands are represented by darker blue tones, which indicate shorter tree heights and open canopy stands. The pockets of darker red pixels represent mature forest, composed of taller tree heights and closed canopy stands. Most of the coniferous forest in this region ranges from 12 to 18 m heights with partly closed stand canopies.

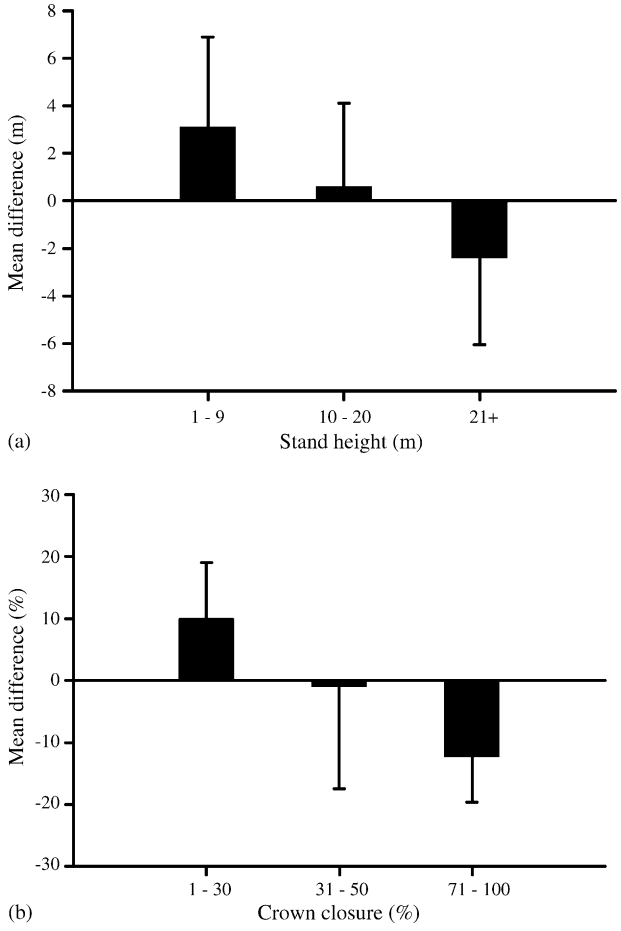

Fig. 6. Distribution of prediction differences using ETM+ data for (a) stand height and (b) crown closure based on the validation sample. The vertical bars show the mean difference computed as predicted subtracted from actual values for three classes. The error bars represent the standard deviation.

and underestimated at the high end for stand height greater than 20 m and greater than 70% crown closure (Fig. 6a and b). While these values were similar to other reported studies (Gerylo et al., 2002), the consequence of these results could manifest itself in the AGB and stand volume estimations.

3.4. Mapping of aboveground biomass and stand volume

Lower biomass values were observed in cutblocks and regenerating stands, and patterns of increasing biomass (Fig. 7) were visible in areas where stand height and crown closure values were also increasing (Fig. 5).

Based on the validation sample, the average difference in BioSTRUCT estimated AGB from the segmented 3×3 window was lower, less variable, and more statistically similar to the field values ($\bar{X} = -4.0$ tonnes/ha, $S = 47.8$ tonnes/ha, $p = 0.609$) compared to its estimate from the full 3×3 image window ($\bar{X} = -23.4$ tonnes/ha, $S = 76.2$ tonnes/ha, $p = 0.066$). This result is significant as AGB from BioSTRUCT with image segmentation approximated values derived independently from the field more so than from sampling the full 3×3 image window. These results were also within the range of values reported by Fazakas et al. (1999), Tomppo et al. (2002), Zheng et al. (2004), and Luther et al. (in press).

Similar to AGB results, stand volume from the segmented 3×3 window using BioSTRUCT was closer to field values than from sampling the entire 3×3 window. The average difference in Landsat ETM+ estimated stand volume from the segmented 3×3 window was lower, less variable, and more statistically similar to the field validation sample ($\bar{X} = -3.6$ m^3/ha, $S = 48.5$ m^3/ha, $p = 0.650$) compared to its estimate from the full 3×3 image window ($\bar{X} = -17.7$ m^3/ha, $S = 63.2$ m^3/ha, $p = 0.139$). Further, the BioSTRUCT AGB

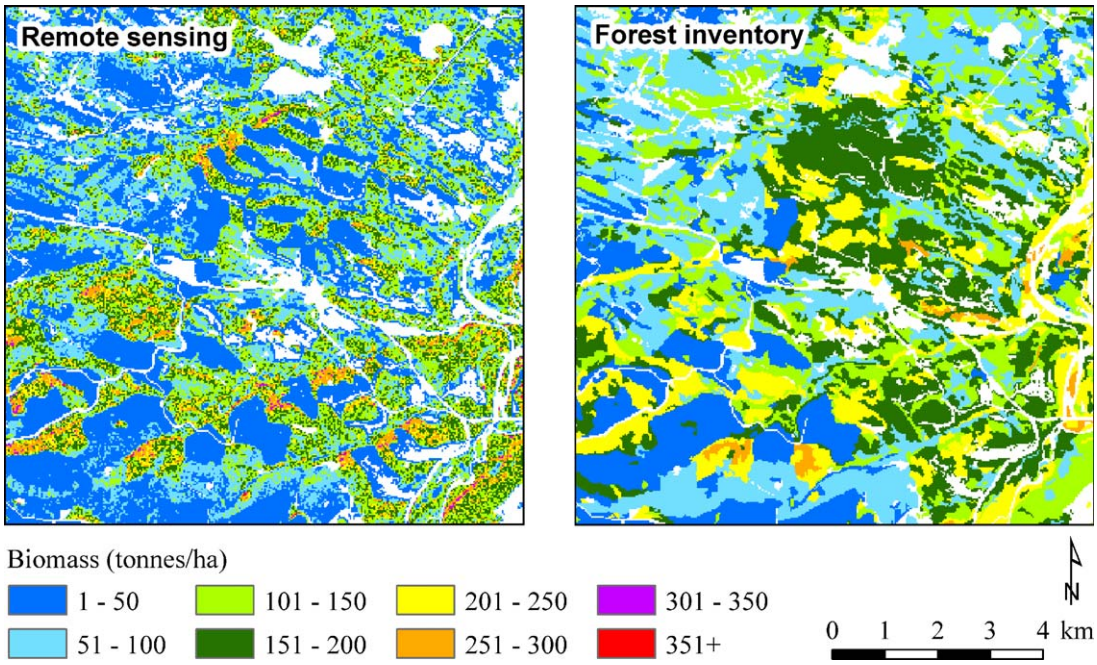

Fig. 7. Comparison of biomass (tonnes/ha) estimates generated from BioSTRUCT and forest inventory. It is visibly evident in the remotely sensed image that recent harvesting activities occurred, as shown in the upper central area by the lower (dark blue) biomass estimates. The forest inventory is out-dated in this region since higher (dark green) biomass estimates representing mature forest still exist.

and stand volume was modeled with the validation data set and found to be linear with an adjusted R^2 and RMSE values of 0.65 and 37.6 tonnes/ha, and 0.69 and 70.0 m^3/ha, respectively. These AGB values from the validation data were similar to R^2 values of 0.67 reported by Zheng et al. (2004) and 0.54–0.68 reported by Coulibaly et al. (2003).

The AVI biomass and volume estimates were statistically different when compared to the validation sample (biomass: $\bar{X} = -27.6$ tonnes/ha, $S = 71.8$ tonnes/ha, $p = 0.023$; volume: $\bar{X} = -56.0$ m^3/ha, $S = 132.9$ m^3/ha, $p = 0.013$). These average differences were approximately larger than 7× for biomass and 15× for volume, a large difference from biomass carbon stocks and volume perspectives. The AVI biomass and volume estimates were also more variable than those derived using BioSTRUCT and the Landsat image models. The AVI provincial inventory for the study area was 9–10 years older

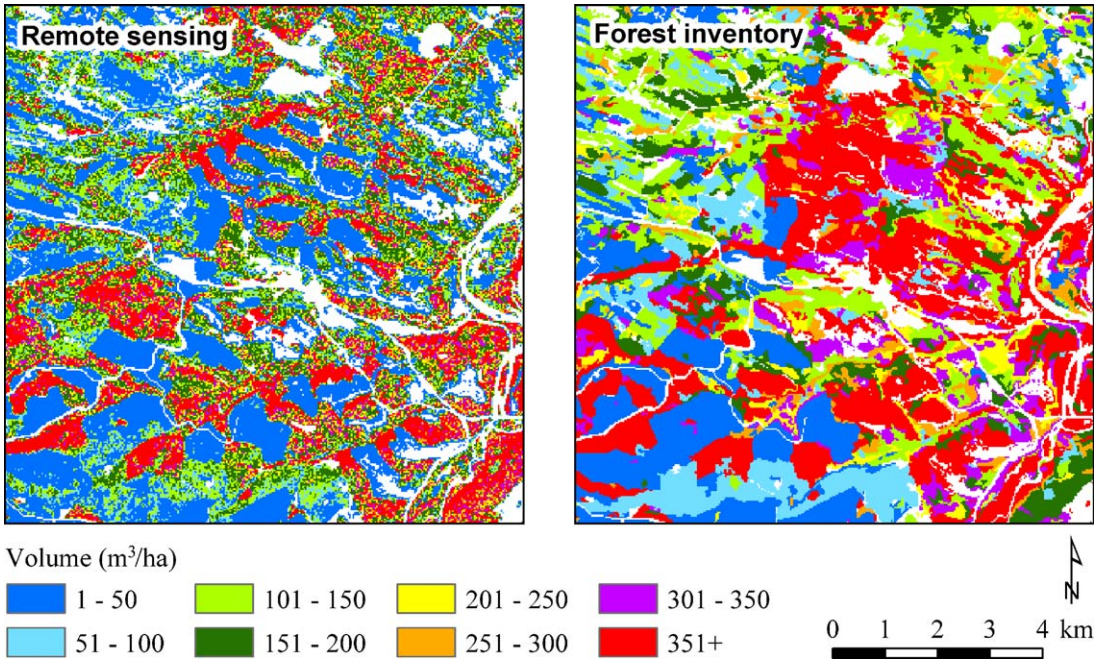

Fig. 8. Comparison of volume (m^3/ha) estimates generated from BioSTRUCT and forest inventory. In the recently harvested areas, cutblocks are not evident in the forest inventory image but are characterized in the remotely sensed image by the lower (dark blue) volume estimates.

than the satellite image resulting in harvesting patterns that were visible on the image but not on the map (Figs. 7 and 8). These observations explain, in part, the larger biomass and volume estimates from the AVI compared to the image.

4. Discussion

4.1. Study advancements and forest management implications

Two advancements are reported in this study. First, the fundamental basis of BioSTRUCT, was to use the image models of stand attributes, stand height, and crown closure, as inputs to an inventory-based model that estimates AGB and stand volume. This approach is consistent with the EOSD approach of using structure to estimate biomass (Luther et al., 2002), particularly since it is very difficult to estimate AGB directly based on spectral response data from the optical portion of the electromagnetic spectrum (Franklin, 2001). Results from direct estimation of AGB and stand volume were similar to previous studies (Fazakas et al., 1999; Tomppo et al., 2002), and less favourable than those from BioSTRUCT. Thus, efforts directed at improving the image estimates of stand height and crown closure would directly result in improvements toward estimating AGB and stand volume. Second, image segmentation was introduced as an approach to improve the relationships between the Landsat ETM+ image and stand attributes of height and crown closure. Two of the more relatively successful approaches have been the use of continuous variable models, as applied in this study, and non-parametric *k*-nearest neighbours (Cohen et al., 2001; Franco-Lopez et al., 2001; Mäkelä and Pekkarinen, 2004). Both of these approaches rely on the availability of well-positioned field plot data from which its associated spectral response values are extracted from the image and used in modeling. Because the accurate location of a field plot on the image is extremely difficult due to possible errors in the field-based positional coordinates and from residual errors in rectifying a satellite image onto a map, an image window is often used rather than sampling a single pixel (Halme and Tomppo, 2001). The bias from estimating stand volumes of conifer species has been shown to be lower when sampling in a window compared to sampling a single pixel (Halme and Tomppo, 2001). Image segmentation proved to be a significant refinement to the image modeling process as it resulted in more suitable data for the estimation of stand variables, consistent with results reported by Mäkelä and Pekkarinen (2001). Both AGB and stand volume estimates were statistically similar to the validation sample when image segmentation was used to sample image values compared to sampling pixels within a full 3×3 window. Similar to other published studies, BioSTRUCT tended to underestimate AGB at high biomass values and overestimate AGB at low values (Zheng et al., 2004; Luther et al., in press).

The forest management implications of BioSTRUCT for estimating biomass carbon stocks or total volume appear to be significant. Over the study area (~260 000 ha), biomass estimated from extending the field plots was 23.9 million tonnes, from BioSTRUCT it was 25.6 million tonnes, and from the AVI, biomass was estimated to be 33.7 million tonnes. Similarly, estimated total volume from field plots was 42.5 million m^3, from BioSTRUCT it was 46.6 million m^3, and from the AVI, volume was computed to be 61.3 million m^3. BioSTRUCT estimates and those from field plots was less than 10%, whereas the difference was larger than 40% when using the AVI; this is a significant figure if statements pertaining to the amount of potential biomass carbon stocks or total volume were to be made. While sample plots can be used to derive AGB and volume estimates over an area, they do not provide information about spatial distribution over the landscape (e.g., Figs. 7 and 8), which is an important advantage from using remote sensing data.

4.2. Data and error considerations

This study integrated inventory plot data and remote sensing models into BioSTRUCT for AGB and stand volume estimation and mapping. To build from this study, field plot distribution and error propagation were identified as factors that influenced both the results that were obtained, and the degree to which this approach could be applied over larger areas.

The PGS plot distribution was mostly labeled as the coniferous species group, since this was the dominant species type in the study area. Applying the BioSTRUCT method to estimate AGB and stand volume for coniferous, deciduous, and mixed species groups will be necessary in order for the method to be of application value to the forest inventory, management, and carbon accounting communities.

Tree and stand measurement errors, modeling, and image processing, including both pre-processing and classification procedures, together result in unknown errors and statistical variation in model parameter estimation and mapping. While the propagation of errors introduced from the various data sources, models, and procedures applied are beyond the scope of this paper, acknowledging their sources is a first step towards its resolution. The two primary sources of error are those associated with the field plot and spatial inventory data and models of AGB and stand volume; and those associated with image pre-processing (e.g., atmospheric correction and orthorectification), image modeling of stand structure, and land cover classification from which to apply the modeled biomass and volume values. Notably, deriving values of actual measurement errors whether it be field or image, is often difficult and must be estimated when data are collected from multiple sources. Research will need to analyze the practical sources of error and how they propagate to determine the overall uncertainty in the estimation and mapping of AGB and stand volume from literature reported by Bevington (1969), Chave et al. (2004), Phillips et al. (2000), and others.

5. Conclusions and future initiatives

Both hypotheses were supported by results generated in this study. BioSTRUCT combines continuous variable modeling of stand structure from the Landsat ETM+ image with image

segmentation for pixel sampling that was applied to both AGB and stand volume estimation and mapping. BioSTRUCT resulted in estimates that were statistically similar to independent validation data, and provided estimates that were more reflective of current conditions on the landscape than those based on AVI data (i.e., spatial inventory) alone.

Future work to expand the biomass and volume estimates to a larger area entails consideration of sensor platform, extension of model application, and normalization procedures. While this study relied on use of Landsat data because of its predominant use in EOSD (Luther et al., 2002; Wulder et al., 2003), failure of the Scan Line Corrector onboard Landsat 7 (Maxwell, 2004) and the near end life of Landsat 5 will entail consideration of other sensors. Previous studies, for example, have reported models of stand height and volume with R^2 values that were higher from Spot than from Landsat (Hyyppä et al., 2000). Future work will entail evaluation of other sensors should Landsat data not be available in future.

Larger area application requires transferring the model coefficients to adjacent scenes. Several factors influence the remote sensing estimates from scene-to-scene, such as confirmation of model form, phenological differences, and atmospheric conditions. Therefore, further attention to these issues would be necessary before the model form and model coefficients could be applied to other image scenes. The non-linear relationship between stand attributes and remote sensing reflectance values was considered reasonable because it follows the successional trend of growth for most forest species. At the seedling stage, tree height initially increases slowly until it is well established, from which follows a period of more rapid growth until it tapers off as maturity is reached (Avery and Burkhart, 2002, p. 338). This non-linear spectral pattern of succession has been reported in other studies that have been explained by the influence of canopy development, amount of shadow within the canopy, and forest understory effects on spectral response (Nilson and Peterson, 1994; Jakubauskas, 1996; Song et al., 2002). Thus, while the model form used in this study appears reasonable, confirmation of model coefficients would entail refitting the model with a larger sample of plots representing a geographically larger area for a full range of coniferous, deciduous and mixedwood species. To minimize the influence of vegetative phenology and the atmosphere, normalization procedures are in development. Standardizing the data collection and pre-processing procedures will involve: (1) acquiring near-anniversary date imagery and then applying radiometric normalization procedures, and (2) geographically stratifying the imagery by ecozone to reduce spectral variability of forest stands within different ecosystems. The results for conifer species were highly encouraging given that over the area sampled, image estimates were statistically similar to field plot values. Consistent with Mäkelä and Pekkarinen (2004), the methods developed in this study are intended for models that estimate AGB and stand volume in areas where no other forest information is available. Once the field and image models have been developed, they may be applied to other ecologically similar areas. Addressing the data and error considerations identified in this study will further refine BioSTRUCT towards increasing its applicability over larger areas. Within the framework of EOSD and national implementation, BioSTRUCT is one of several methods that have been developed, with the intent to use the method that best matches the types of data available.

Acknowledgements

This study was part of the Earth Observation for the Sustainable Development of Forests (EOSD) initiative (http://www.pfc.forestry.ca/eosd/index_e.html). We thank our Natural Resources Canada, Canadian Forest Service colleagues Joan Luther, André Beaudoin, and Richard Fournier (Université de Sherbrooke), for joint development of methods on biomass mapping. Reviews of the manuscript by Joan Luther prior to journal submission, and by three anonymous journal reviewers are gratefully acknowledged. Funding and support for this project were provided by the Canadian Space Agency, Natural Resources Canada, Canadian Forest Service for EOSD, and by David Price for the Ecoleap-West study funded by the Foothills Model Forest, Prairie Adaptation Research Cooperative, and Network Centres of Excellence—Sustainable Forest Management. Assistance in modeling was provided by Yonghe Wang, Natural Resources Canada. We thank H. Lougheed Weldwood of Canada (now Hinton Wood Products) for provision of AVI and inventory plot data. A portion of the continuous crown closure data was provided by G. McDermid of the University of Calgary and S.E. Franklin of the University of Saskatchewan.

References

Achuff, P.I., 1992. Natural Regions, Subregions and Natural History Themes of Alberta: a Classification for Protected Areas Management. Alberta Environmental Protection, Edmonton, Alta., Canada.

Alberta Environmental Protection, 1991. Alberta Vegetation Inventory Standards Manual Version 2.1. Alberta Environmental Protection, Resource Data Division, Data Acquisition Branch, Edmonton, Alta..

Avery, T.E., Burkhart, H.E., 2002. Forest Measurements, fifth ed. McGraw-Hill, New York, NY, pp. 337–339.

Bevington, P.R., 1969. Data Reduction and Error Analysis for the Physical Sciences. McGraw-Hill Book Company Inc., New York, NY.

Bonner, G.M., 1985. Inventory of Forest Biomass in Canada. Petawawa National Forestry Institute, Canadian Forest Service, Ontario, Canada.

Brown, S.L., Schroeder, P., Kern, J.S., 1999. Spatial distribution of biomass in forests of the eastern USA. Forest Ecol. Manage. 123, 81–90.

Brown, S., 2002. Measuring carbon in forests: current status and future challenges. Environ. Pollut. 116, 363–372.

Chave, J., Condit, R., Aguilar, S., Hernandez, A., Lao, S., Perez, R., 2004. Error propagation and scaling for tropical forest biomass estimates. Philos. Trans. R. Soc. Lond. B 359, 409–420.

Cohen, W.B., Maiersperger, T.K., Spies, T.A., Oetter, D.R., 2001. Modeling forest cover attributes as continuous variables in a regional context with Thematic Mapper data. Int. J. Remote Sensing 22, 2279–2310.

Coulibaly, L., Adégbidi, H., Sérélé, C., 2003. Mapping forest biomass: towards an approach using ecological parameters and remote sensing. In: 25th Canadian Symposium on Remote Sensing. Montréal, Qué., Canada, 14–17 October 8 p.

Crow, T.R., Laidly, P.R., 1980. Alternative models for estimating woody plant biomass. Can. J. Forest Res. 10, 367–370.

Definiens Imaging, 2002. eCognition Software: Release 3.0. Definiens Imaging GmbH, Munich, Germany.

Dong, J., Kaufmann, R.K., Myneni, R.B., Tucker, C.J., Kauppi, P.E., Liski, J., Buermann, W., Alexeyev, V., Hughes, M.K., 2003. Remote sensing estimates of boreal and temperate forest woody biomass: carbon pools, sources, and sinks. Remote Sensing Environ. 84, 393–410.

Fazakas, Z., Nilsson, M., Olsson, H., 1999. Regional forest biomass and wood volume estimation using satellite data and ancillary data. Agricult. Forest Meteorol. 98–99, 417–425.

Fournier, R., Luther, J., Guindon, L., Lambert, M.-C, Piercey, D., Hall, R.J., Wulder, M., 2003. Mapping aboveground tree biomass at the stand level from inventory information: test cases in Newfoundland and Quebec. Can. J. Forest Res. 33, 1846–1863.

Franco-Lopez, H., Ek, A.R., Bauer, M.E., 2001. Estimation and mapping of forest stand density, volume and cover type using the *k*-nearest neighbours method. Remote Sensing Environ. 77, 251–274.

Franklin, S.E., 2001. Remote Sensing for Sustainable Forest Management. Lewis Publishers, CRC Press Inc., New York, NY.

Franklin, S.E., Peddle, D.R., Dechka, J.A., Stenhouse, G.B., 2002. Evidential reasoning with Landsat TM, DEM and GIS data for landcover classification in support of grizzly bear habitat mapping. Int. J. Remote Sensing 23, 4633–4652.

Gemmell, F.M., 1995. Effects of forest cover, terrain, and scale on timber volume estimation with Thematic Mapper data in a Rocky Mountain site. Remote Sensing Environ. 51, 291–305.

Gerylo, G.R., Hall, R.J., Franklin, S.E., Smith, L., 2002. Empirical relations between Landsat TM spectral response and forest stands near Fort Simpson, Northwest Territories, Canada. Can. J. Remote Sensing 28, 68–79.

Gillis, M.D., Leckie, D.G., 1993. Forest inventory mapping procedures across Canada. Canadian Forest Service, Petawawa National Forest Institute Information Report, PI-X-114.

Hall, R.J., Davidson, D.P., Peddle, D.R., 2003. Ground and remote estimation of leaf area index in Rocky Mountain forest stands, Kananaskis, Alberta. Can. J. Remote Sensing 29, 411–427.

Halme, M., Tomppo, E., 2001. Improving the accuracy of multisource forest inventory estimates by reducing plot location error—a multicriteria approach. Remote Sensing Environ. 78, 321–327.

Hansen, M.J., Franklin, S.E., Woudsma, C., Peterson, M., 2001. Forest structure classification in the North Columbia mountains using the Landsat TM Tasseled Cap wetness component. Can. J. Remote Sensing 27, 20–32.

Harrell, P.A., Bourgeau-Chavez, L.L., Kasischke, E.S., French, N.H.F., Christensen, N.L., 1995. Sensitivity of ERS-1 and JERS-1 RADAR data to biomass and stand structure in Alaskan boreal forest. Remote Sensing Environ. 54, 247–260.

Huang, S., 1994. Individual Tree Volume Estimation Procedures for Alberta: Methods of Formulation and Statistical Foundations. Land and Forest Service, Alberta Environmental Protection, Tech. Rep. Pub. No. T/288, Edmonton, Alta., 80 pp.

Huang, C., Wylie, B., Homer, C., Yang, L., Zylstra, G., 2002. Derivation of a Tasseled cap transformation based on Landsat 7 at-satellite reflectance. Int. J. Remote Sensing 23, 1741–1748.

Hyyppä, J., Hyyppä, H., Inkinen, M., Enghahl, M., Linko, S., Zhu, Y.-H., 2000. Accuracy comparison of various remote sensing data sources in the retrieval of forest stand attributes. Forest Ecol. Manage. 128, 109–120.

Jakubauskas, M.E., 1996. Thematic Mapper characterization of lodgepole pine seral stages in Yellowstone National Park, USA. Remote Sensing Environ. 56, 118–132.

Jakubauskas, M.E., Price, K.P., 1997. Empirical relationships between structural and spectral factors of Yellowstone lodgepole pine forests. Photogram. Eng. Remote Sensing 63, 1375–1381.

Jenkins, J.C., Chojnacky, D.C., Heath, L.S., Birdsey, R.A., 2003. National-scale biomass estimators for United States tree species. Forest Sci. 49, 12–35.

Kasischke, E.S., Bourgeau-Chavez, L.L., Christensen, N.L., Haney, E., 1994. Observations on the sensitivity of ERS-1 SAR image intensity to changes in aboveground biomass in young loblolly pine forests. Int. J. Remote Sensing 15, 3–16.

Kurz, W.A., Apps, M.J., 1999. A 70-year retrospective analysis of carbon fluxes in the Canadian forest sector. Ecol. Appl. 9, 526–547.

Landgrebe, D.A., 2000. Information extraction principles and methods for multispectral and hyperspectral image data. In: Chen, C.H. (Ed.), Information Processing for Remote Sensing. World Scientific Publishing Company, New Jersey, pp. 3–38.

Lee, N.J., Nakane, K., 1997. Forest vegetation classification and biomass estimation based on Landsat TM data in a mountainous region of west Japan. In: Gholz, H.L., Nakane, K., Shimoda, H. (Eds.), The Use of Remote Sensing in the Modeling of Forest Productivity. Kluwer, Dordrecht, pp. 159–171.

Luther, J.E., Fournier, R.A., Hall, R.J., Ung, C.-H., Guindon, L., Piercey, D.E., Lambert, M.-C., Beaudoin, A., 2002. A strategy for mapping Canada's forest biomass with Landsat TM imagery. In: Proceedings of the International Geoscience and Remote Sensing Symposium/24th Canadian Symposium on Remote Sensing, Toronto, Ont., Canada, 24–28 June, pp. 1312–1315.

Luther, J.E., Fournier, R.A., Piercey, D.E., Guindon, L., Hall, R.J. Biomass mapping using forest type and structure derived from Landsat TM imagery. Int. J. Appl. Earth Observ. Geoinform., in press.

Mäkelä, H., Pekkarinen, A., 2001. Estimation of timber volume at the plot level by means of image segmentation and Landsat TM imagery. Remote Sensing Environ. 77, 66–75.

Mäkelä, H., Pekkarinen, A., 2004. Estimation of forest stand volumes by Landsat TM imagery and stand-level field-inventory data. Forest Ecol. Manage. 196, 245–255.

Manning, G.H., Massie, M.R.C., Rudd, J., 1984. Metric Single-Tree Weight Tables for the Yukon Territory. Information Report BC-X-250. Canadian Forest Service, Pacific Forest Centre, Victoria, BC.

Markham, B., Barker, J., 1986. Landsat MSS and TM post calibration dynamic ranges, exoatmospheric reflectances and at satellite temperature. EOSAT Landsat Tech. Notes 1, 3–7.

Maxwell, S., 2004. Filling Landsat ETM+ SLC-off gaps using a segmentation model approach. Photogram. Eng. Remote Sensing 70, 1109–1111.

Nilson, T., Peterson, U., 1994. Age dependence of forest reflectance: analysis of main driving factors. Remote Sensing Environ. 48, 319–331.

Oakdale Engineering, 2002. DataFit version 8.0.32. Oakdale, PA, USA.

Parresol, B.R., 1999. Assessing tree and stand biomass: a review with examples and critical comparisons. Forest Sci. 45, 573–593.

Peddle, D., Teillet, P., Wulder, M., 2003. Radiometric image processing. In: Wulder, M., Franklin, S. (Eds.), Remote Sensing of Forest Environments: Concepts and Case Studies. Kluwer Academic Publishers, Boston, pp. 181–208.

Penner, M., Power, K., Muhairwe, C., Tellier, R., Wang, Y., 1997. Canada's Forest Biomass Resources: Deriving Estimates from Canada's Forest Inventory. Natural Resources Canada, Canadian Forest Service, Pacific Forestry Centre, Victoria, BC. Information Report BC-X-370, 33 pp.

Philip, M.S., 1994. Measuring Trees and Forests, second ed. CABI Publishing, New York, NY.

Phillips, D.L., Brown, S.L., Schroeder, P.E., Birdsey, R.A., 2000. Toward error analysis of large-scale forest carbon budgets. Global Ecol. Biogeogr. 9, 305–313.

Price, D.T., Peng, C.H., Apps, M.J., Halliwell, D.H., 1999. Simulating effects of climate change on boreal ecosystem carbon pools in central Canada. J. Biogeogr. 26, 1237–1248.

Sader, S.A., Waide, R.B., Lawrence, W.T., Joyce, A.T., 1989. Tropical forest biomass and successional age class relationships to a vegetation index derived from Landsat TM data. Remote Sensing Environ. 28, 71–89.

Singh, T., 1982. Biomass Equations for Ten Major Tree Species of the Prairie Provinces. Canadian Forest Service, Northern Forest Centre, Edmonton, Alta. Information Report NOR-X-242.

Singh, T., 1984. Biomass Equations for Six Major Tree Species of the Northwest Territories. Canadian Forest Service, Northern Forest Centre, Edmonton, Alta. Information Report NOR-X-257.

Song, C., Woodcock, C.E., Li, X., 2002. The spectral/temporal manifestation of forest succession in optical imagery. The potential of multitemporal imagery. Remote Sensing Environ. 82, 285–302.

Teillet, P.M., Fedosejevs, G., 1995. On the dark target approach to atmospheric correction of remotely sensed data. Can. J. Remote Sensing 21, 374–387.

Ter-Mikaelian, M., Korzukhin, M., 1997. Biomass equations for sixty-five North American tree species. Forest Ecol. Manage. 97, 1–24.

Tiwari, A.K., 1994. Mapping forest biomass through digital processing of IRS-1A data. Int. J. Remote Sensing 15, 1849–1866.

Tomppo, E., Nilsson, M., Rosengren, M., Aalto, P., Kennedy, P., 2002. Simultaneous use of Landsat-TM and IRS-1C WiFS data in estimating large area tree stem volume and aboveground biomass. Remote Sensing Environ. 82, 156–171.

Trotter, C.M., Dymond, J.R., Goulding, C.J., 1997. Estimation of timber volume in a coniferous plantation forest using Landsat TM. Int. J. Remote Sensing 18, 2209–2223.

Wang, J.R., Zhong, A.L., Kimmins, J.P., 2002. Biomass estimation errors associated with the use of published regression equations of paper birch and trembling aspen. Northern J. Appl. Forestry 19, 128–136.

Wang, Y., Kasischke, E.S., Melack, J., Davis, F.W., Christensen, N.L., 1994. The effects of changes in loblolly pine biomass and soil moisture on ERS-1 SAR backscatter. Remote Sensing Environ. 49, 25–31.

Weldwood of Canada Limited Hinton Division, 1999. Weldwood Permanent Growth Samples—The Manual. Version 6.99. Hinton, Alta., Canada.

Wood, J.E., Gillis, M.D., Goodenough, D.G., Hall, R.J., Leckie, D.G., Luther, J.E., Wulder, M.A., 2002. Earth observation for sustainable development of forests: project overview. In: Proceedings of the International Geoscience and Remote Sensing Symposium/24th Canadian Symposium on Remote Sensing, Toronto, Ont., 24–28 June, pp. 1299–1302.

Wulder, M.A., Dechka, J., Gillis, M., Luther, J., Hall, R.J., Beaudoin, A., Franklin, S.E., 2003. Operational mapping of the land cover of the forested area of Canada with Landsat data: EOSD land cover program. Forestry Chron. 79, 1075–1083.

Zheng, D., Rademacher, J., Chen, J., Crow, T., Bresee, M., Le Moine, J., Ryu, S.-R., 2004. Estimating aboveground biomass using Landsat 7 ETM+ data across a managed landscape in northern Wisconsin, USA. Remote Sensing Environ. 93, 402–411.